State-Space Model Representation to Characterize an Energy-Harvesting Circuit

Regis Rousseau, Guillaume Villemaud, and Florin Hutu

Abstract – This paper presents a method to model an energy-harvesting circuit and a propagation channel as parts of a wireless power transfer (WPT) system. Previously, an original solution was proposed by the authors to maximize the collected dc power level, implying modeling the different parts of the system by using state-space representation and using convex optimization algorithms to calculate multicarrier signal weights. First, a state-space model of the radio channel is obtained using the multivariable output-error state space (MOESP) algorithm. With the vector-fitting method a state-space representation is obtained to model the linear part of the energy-harvesting circuit. Last, with the polynomial-nonlinear state-space (PNLSS) method, the nonlinear part of the rectifier is also modeled.

1. Introduction

For several years now, research has been undertaken to maximize the dc harvested power obtained with an energy-harvesting circuit. The use of multitone signals has shown their impact in terms of increasing performance. This article presents the scientific advances in this field and the challenges for tomorrow [1]. In the case of power transfer, [2] has shown that the use of power-optimized waveform (POW) considerably impacts the efficiency of the rectifier. With an optimal range of the subcarrier spacing, the voltage ripple, and the total number of subcarriers, a relationship has been established to maximize the efficiency of a single-shunt rectifier. POW is a solution to increase the peak-to-average power ratio (PAPR) of the transmitted source signal and thus to deliver more power to the load. Since peaks of high power drive the rectifier with a much higher efficiency than the average low-level input, they contribute more to the output dc voltage. But some trade-offs appear, such as the frequency spacing between subcarriers and their number regarding the bandwidth of matching network.

However, this concerns only the rectifier's physical characteristics. Nowadays, the trend is also to take into account the transmission channel's characteristics. The radio-frequency source (multi-sine), the channel, and the rectifier are considered as a global WPT system. The authors in [3] described the influence of a realistic channel on the WPT system's overall efficiency. The presented measurements show that the power conversion efficiency (PCE) is always better in the case of a single-path channel. On the other hand, having a precise knowledge of the channel, such as the coherence bandwidth, will be crucial in the choice of the number of tones and the frequency bandwidth of the transmitted RF signal.

Waveform tailoring algorithms according to the characteristics of the propagation channel have thus been developed [4] and experimentally verified [5]. In these study cases, the rectifier consists of only a model based on the I-V characteristic law of a Schottky diode [6]. Other works concern rectifier model extraction based on curve fitting [7]. The dc output power as a function of RF input level is measured, and this characteristic is approximated from simulation data using a data-fitting tool. Several nonlinear curve-fitting models are currently used, such as a second-order polynomial model, sigmoid model, and rational function model. In these solutions, the rectifier is considered ideal and depends only on the model of Schockley's law or is modeled by a neighboring polynomial. Those adaptive and optimized waveforms use nonconvex optimization problems, and therefore the implementation is complex.

In this paper, we describe a possible way of closed loop modeling of a WPT system by using linear and nonlinear state-space models. The use of convex optimization algorithms will be employed to maximize the dc power harvested in a WPT scenario. Three main aspects of a WPT system are taken into account: the RF multi-sine source, the propagation channel, and the rectifier in its entirety. Each of its elements finds its representation in a state-space model, and the algorithm optimization will become a convex optimization resolution. This work describes different algorithms to represent with a state-space model a global system of WPT. The first part shows the global system and the goal of this approach, the second part shows the state-space model of a frequency-selective channel knowing the channel state information, and the last part describes the state-space model of the linear and nonlinear part of the rectifier.

2. Global System Model

The initial scenario foresees a wireless power supply from a source to a connected object equipped with a rectenna that will ensure the charging of an external storage element (battery or super-capacitor). This study case rather provides a scenario of an indoor condition with non-line-of-sight (NLOS) or line-of-sight (LOS) environments and with short distances (a

Manuscript received 28 August 2020.

Regis Rousseau, Guillaume Villemaud, and Florin Hutu are with INSA Lyon, CITI laboratory-INRIA, 6 avenue des arts, F-69621 Villeurbanne, France; e-mail: regis.rousseau@insa-lyon.fr, guillaume.villemaud@insa-lyon.fr, florin-doru.hutu@insa-lyon.fr.

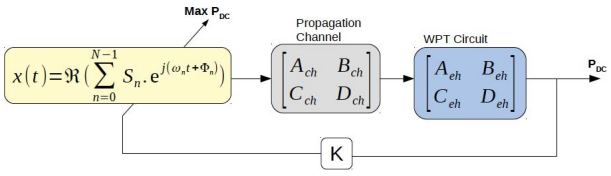

Figure 1. A WPT system seen as a closed loop. Propagation channel and rectifying circuit are modeled by their respective state-space models.

few meters). As detailed in [8], the global system is seen as a closed-loop WPT system and is put in the form presented in Figure 1. The channel is considered to be linear, and the rectifier, by the presence of the rectifying diode, is considered to be nonlinear, so their models do not use the same shaping algorithm and are thus treated distinctly.

Before generating the adaptive waveform, the RF source generates a reference orthogonal frequency-division multiplexing (OFDM) signal to know the channel estimation in amplitude and phase. Knowing beforehand the electrical characteristics of the rectifier and putting them in a form of the state-space model, an algorithm computes the channel state information on the state-space model. A closed loop is created, and an optimized waveform can be generated.

3. Frequency-Selective Channel Model

First, a static wireless multipath channel between the source and the rectifier is simulated. As mentioned in [3], the source node transmits multi-sine signals to the receiver via a multipath channel with gain β_k and delay τ_k for the k_{th} path. Starting from this, we assume that the transmitter, receiver, and channel environment are stationary during the observation time. The considered frequency-selective channel corresponds to a NLOS channel power delay profile scenario with a root-mean-square (RMS) delay spread of 100 ns, coherence bandwidth of 5 MHz, and terminal speed of 3 m/s (equivalent to a channel model B for HYPERLAN/2 [9]).

The channel estimator process uses a block-pilot based technique. Leveraging channel estimation for OFDM, we can therefore collect the channel state information (CSI) on each frequency. The pilot-based technique uses a reference pilot signal that the transmitter and the receiver both know. The channel status information can be calculated from a comparison between the received signal and known reference signal at the receiver. Pilot symbols are allocated one frequency out of two. Also, we use a least-square (LS) method to calculate the CSI because of its low complexity. Our channel estimation system operates at 2.45 GHz center frequency with a 20 MHz bandwidth and 256 subcarriers, corresponding to a subcarrier spacing of 78.125 kHz. However, the upper and lower 5 MHz bands are used as guard bands, and the region that is actually used to estimate the channel is the middle one of 10 MHz.

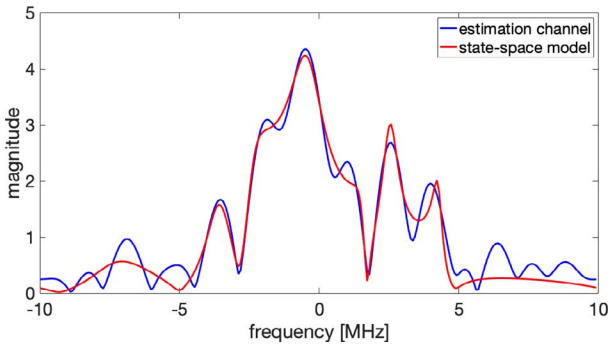

Figure 2. Magnitude of the frequency response from impulse response of the estimated channel (blue) and from the MOESP method with order 10 (red). The bandwidth of the channel is 20 MHz with a 10 MHz guard band.

From the simulated input/output of the channel, the state-space model is computed with a system identification based on Multivariable Output-Error State sPace (MOESP). MOESP is a deterministic method to identify linear time-invariant systems. The developed MOESP method cited in [10] is based on the LQ decomposition of Hankel matrix formed from input/output data, where L is the lower triangular matrix and Q is the orthogonal one. A singular value decomposition (SVD) can be performed on a block from the L matrix to obtain the system order and the extended observability matrix. From this matrix, it is possible to estimate the matrices C and A of state-space model. The final step is to solve overdetermined linear equations using the least-square method to calculate matrices B and D. Figure 2 shows the comparison of the magnitude of the frequency response of the wireless channel from CSI and the magnitude of the frequency response from a space-state model. The RMS frequency response error of the MOESP model on the estimation data is 0.5908.

4. Rectifier Model

Since the forecast scenario concerns very low received powers (approx. –40 dBm), a rectifier with a single diode was retained. The single shunt diode rectifier circuit was designed using a Skyworks SMS7630 Schottky diode. The rectifier input was matched to 50 Ω by two L-matching networks (six-order LC bandpass filter). This guarantees an input reflection coefficient between –20 dB and –33 dB for an input signal of 2.45 GHz having a 60 MHz bandwidth and a –20 dBm input power level (all values were optimized and normalized in previous studies). The load resistance is optimized with the same optimization criteria concerning the input reflection coefficient, and its value is 3953 Ω. Table 1 gives reference performance values of this proposed rectifier for a continuous wave (1-tone). The maximum efficiency is obtained for an input power level of –9.5 dBm, and its value is 52.5% for a dc output voltage of 58.91 mV.

Table 1. Voltage and efficiency results

Pin (dBm)	dc voltage (mV)	Efficiency (%)
−40	0.002	1.6
−30	0.089	10
−20	3.613	36
−10	63.195	56

These results are in good agreement with the literature. In [11] an experimental rectifier was presented with a similar rectifier topology. The measured peak efficiencies are, respectively, 4.3%, 24.3%, and 48.5% with an input power level of –30 dBm, –20 dBm, and –10 dBm at a frequency of 2.472 GHz. Therefore our goal is also to maximize dc output voltage for input power below –30 dBm by knowing the distortion of the channel.

4.1 Impedance Matching Network Model

In [8], the authors show that using the vector fitting method, a linear time-invariant system can be computed in a form of a state-space model. A description for the S-parameter based-model is given in [12]. We employed this method to approximate the linear impedance matching network (IMN) seen like a quadripole with a rational function. S-parameters of IMN (six-order LC bandpass filter) can then be modeled as a sum of the residues, r_k, over first-order poles, $p_n : H(s) = \sum_{k=1}^{N} \frac{r_k}{s-p_k} + d = C(s \cdot \mathbb{I} - A)^{-1}B + D$, where N denotes the VF order and $s = j\omega$ Considering a two-port ($n = 2$) system and VF of order $N = 5$, the total number of state variables m will be $m = n \cdot N = 10$. Thus, the corresponding state-space model will have the following properties: A is an 10×10 diagonal matrix containing the N poles p_k repeated two times, B is an 10×2 matrix and contains only ones or zeros, C is composed of the r_k residues and is an 2×10 matrix, and D is a 2×2 matrix and is composed of real constants. Figure 3 shows the input reflection coefficient as function of frequency, from 2.4 GHz to 2.5 GHz for $N = 5$ and an input power of –20 dBm. As can be seen, the model for an order of 5 gives a similar response to that of the original model.

4.2 DC Behavior Diode Model

As previously stated, the Schottky diode SMS7630-001LF is selected for the rectifier due to its small series resistance (20 Ω) and its small junction potential (0.34 V). The first step is to model its dc characteristic under reverse bias and forward bias. The objective of this step is to model the nonlinear junction resistance as a polynomial equation. The characteristic was obtained using its electric circuit in the range of –300 mV to +300 mV. Then the dc behavior was represented by a symbolically defined device (SDD) element, which takes the form of a polynomial equation $I_d = f(V_d)$ of order 9, where I_d denotes the current through the diode and V_d denotes the voltage across the diode. Figure 4 shows a comparison of the simulated SPICE model and the polynomial fitting of the I-V characteristic. The correlation is intended to be very good for low voltage values, but beyond 50 mV, an error will appear to be significant as it increases. However, the target values being low, this model can be used since the objective is to recover a low power level at the input of the rectifier.

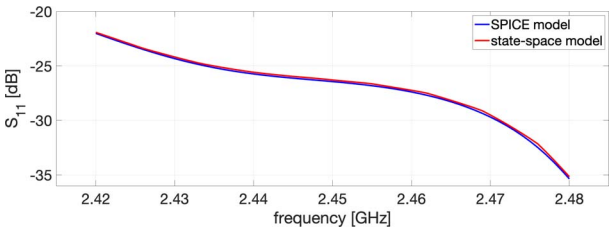

Figure 3. In blue, the reflection coefficient (in decibels) of the original rectifier. In red, the reflection coefficient from VF method, order 5.

4.3 RF Behavior Diode Model

To model the RF behavior of the diode from –300 mV to +300 mV, the nonlinear junction capacitance was also represented by an SDD element. This capacitance value is driven by the voltage Vd across it, based on $C_j = 0.14 \times 10^{-12} e^{(Vd)}$. The same method has been applied to put this equation in the form of a polynomial of order 7. The SDD models a nonlinear voltage-controlled capacitor, whose current can be written $Id = Cj(Vd)\frac{dVd}{dt}$. The time derivative is implemented in the SDD by specifying the weighting function number 1. Figure 5 shows the comparison between the simulated electrical circuit and the simulated polynomial fitting model. This curve shows that the modeling of the nonlinear capacitance of the diode by this exponential function perfectly meets this need for a modeling in polynomial form. The curve resulting from the polynomial model coincides with the original SPICE model over the entire frequency range.

4.4 Polynomial Nonlinear State-Space Model

From now on the rectifier can be entirely modeled by functional blocks given as state-space models. Their state-space model result from the VF methods for the linear parts (impedance matching network and input/

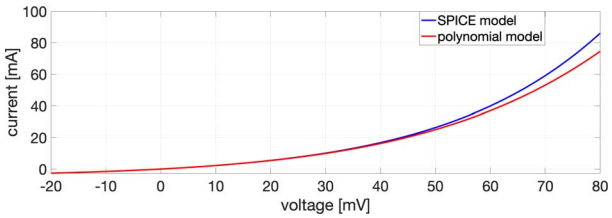

Figure 4. In blue, the original I-V characteristic. In red, the I-V characteristic from polynomial fitting, order 9.

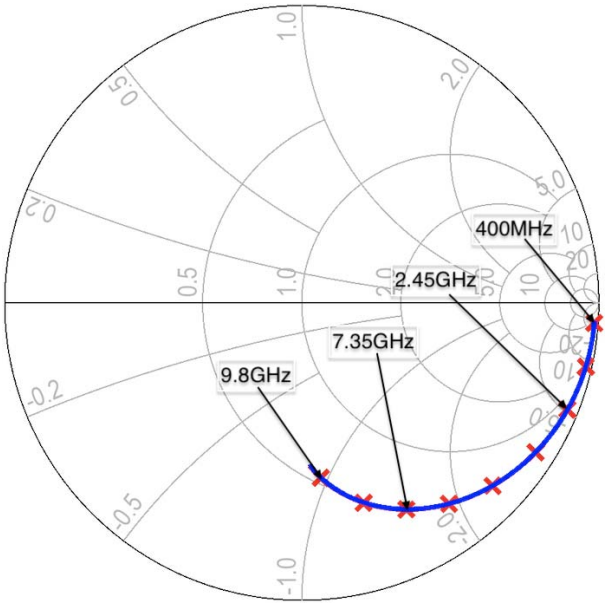

Figure 5. S_{11} parameter for a frequency range from 400 MHz to 9.8 GHz. In blue, the original S_{11} parameter. In red, the obtained polynomial fitting.

output SOT-23 parasitic parts), the nonlinear components being replaced by SDD elements. Figure 6 shows comparison of the rectifier's dc collected voltage as a function of the RF input power between the original rectifier and the fully modeled rectifier. The model is faithful to the original for powers below –20 dBm. Then, while the voltage from the original increases, saturation seems to appear for the rectifier from the models. Nevertheless, our target is the low received power there, so this model is perfectly appropriate for operation below –20 dBm.

The last step to completely model this rectifier with state-space model is to replace these SDD elements with their own nonlinear state-space representation. This representation is carried out with an original method presented in [13] and Matlab functions in [14]. The state and output equations of the model are given by

$$\begin{cases} \dot{x} = A \cdot x + B \cdot u + E \cdot f(x(t), u(t)) \\ y = C \cdot x + D \cdot u + F \cdot g(x(t), u(t)) \end{cases} \quad (1)$$

where $\dot{x}$ is the time derivative operator of the state variable, u is the input vector of length N, and y is the

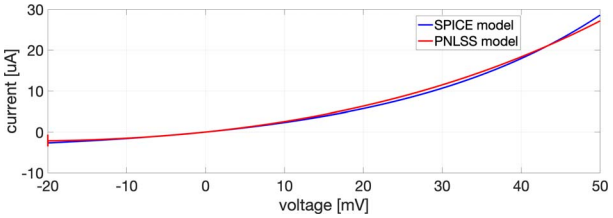

Figure 6. In blue, the original rectifier. In red, the modeled rectifier.

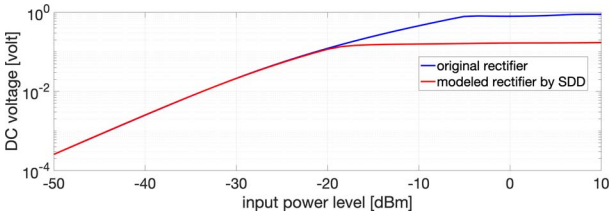

Figure 7. In blue, the original I-V characteristic. In red, the I-V characteristic from PNLSS model, order 2.

corresponding output vector of length P. The state vector has the length N.

The matrix A is the $N \times N$ state matrix, B is the $N \times M$ input matrix, C is the $P \times N$ output matrix, and D is the $P \times N$ feedback matrix. The $f(x(t), u(t))$ and $g(x(t), u(t))$ functions are multivariate and monomial, and the matrices E and F contain the corresponding coefficients. The model is established in three steps: an estimation of the best linear approximation (BLA), an estimation of a subspace model, and an optimization of the model parameters.

Figure 7 shows the output resulting by a dc voltage input from the PNLSS model and the SPICE model. The RMS output error of the best PNLSS model on the estimation data is 2×10^{-5}. However, this error is minimal for weak inputs and tends to increase for larger values. Future work will therefore be needed to improve the precision.

5. Conclusion

This paper proposes strategies to extract state-space representations of the different building blocks of a wireless power transfer system. In more detail, the proposed strategy includes one algorithm to compute a CSI impulse response to a state-space model and two distinct algorithms to compute the linear and nonlinear parts of the rectifier. Future work will focus on putting the state-space model representations in the form of a closed-loop and proposing an optimization algorithm for the adaptive input waveform. Moreover, work will be carried out to reduce the order of the rectifier's model.

6. References

1. COST Action IC1301 Team, "Europe and the Future WPT," *IEEE Microwave Magazine*, **18**, 4, June 2017, pp. 56-87.
2. C. R. Valenta and G. D. Durgin, "Harvesting Wireless Power," *IEEE Microwave Magazine*, **15**, 4, June 2014, pp. 108-120.
3. N. Pan, M. Rajabi, D. Schreurs, and S. Pollin, "Multi-sine Wireless Power Transfer With a Realistic Channel and Rectifier Model," IEEE Wireless Power Transfer Conference, Taipei, Taiwan, May 10–12, 2017, doi: 10.1109/WPT.2017.7953873.
4. B. Clerckx and E. Bayguzina, "Waveform Design for Wireless Power Transfer," *IEEE Transaction on Signal Processing*, **64**, 23, March 2016, pp. 6313-6328.
5. J. Kim, B. Clerckx, and P. D. Mitcheson, "Prototyping

and Experimentation of a Closed-Loop Wireless Power Transmission With Channel Acquisition and Waveform Optimization," IEEE Wireless Power Transfer Conference, Taipei, Taiwan, May 10–12, 2017, doi: 10.1109/WPT.2017.7953827.

6. B. Clerckx, R. Zhang, R. Schober, and D. W. K. Ng, "Fundamentals of Wireless Information and Power Transfer: From RF Energy Harvester Models to Signal and System Designs," *IEEE Journal on Selected Areas in Communications*, **37**, 1, January 2019, pp. 4-33.
7. B. A Mouris, H. Ghauch, R. Thobaben, and B. L. G. Jonsson, "Multi-tone Signal Optimization for Wireless Power Transfer in the Presence of Wireless Communication Links," *IEEE Transactions on Wireless Communications*, **19**, 5, May 2020, pp. 3575-3590. https://ieeexplore.ieee.org/document/9014501
8. R. Rousseau, F. Hutu, and G. Villemaud, "On the Use of Vector Fitting and State-Space Modeling to Maximize the DC Power Collected by a Wireless Power Transfer System," 2nd URSI Atlantic Radio Science Conference, Gran Canaria, Spain, May 28–June 1, 2018, doi: 10.23919/URSI-AT-RASC.2018.8471611. https://ieeexplore.ieee.org/document/9014501
9. J. Medbo and P. Schramm, "Channel Models for HIPERLAN/2 in Different Indoor Scenarios," ETSI EP BRAN 3ERI085B, March 1998, pp. 1-8, doi: 10.1109/TWC.2020.2974950. https://ieeexplore.ieee.org/document/9014501
10. J. N. Juang and M. Q. Phan, *Identification and Control of Mechanical Systems*, Cambridge, England, Cambridge University Press, 2001.
11. Y. Huangl, N. Shinoharal, and H. Toromura, "A Wideband Rectenna for 2.4 GHz-band RF Energy Harvesting," Wireless Power Transfer Conference, Aveiro, Portugal, May 5–6, 2016, doi: 10.1109/WPT.2016.7498816.
12. B. Gustavsen and A. Semlyen, "Rational Approximation of Frequency Domain Responses by Vector Fitting," *IEEE Transaction Power Delivery*, **14**, 3, July 1999, pp. 1052-1061.
13. J. Paduart, L. Lauwers, J. Swevers, K. Smolders, J. Schoukens, and R. Pintelon, "Identification of Nonlinear Systems Using Polynomial Nonlinear State Space Models," *Automatica*, **46**, 4, April 2010, pp. 647-656.
14. K. Tiels, "A Polynomial Nonlinear State-Space Toolbox for Matlab." 21th [sic] IMEKO TC4 International Symposium on Understanding the World Through Electrical and Electronic Measurement, and 19th International Workshop on ADC Modelling and Testing Budapest, Hungary, September 7–9, 2016, pp. 28-31.